Synthesis and Characterization of Polyurethane/Poly(vinylidene chloride) Interpenetrating Polymer Networks

Muneera Begum,[1,2] Siddaramaiah,[1,2] R. Somashekar,[3] H. Somashekarappa[3]

[1]*Department of Chemistry, Sri Jayachamarajendra College of Engineering, Mysore 570 006, India*
[2]*Department of Polymer Science and Technology, Sri Jayachamarajendra College of Engineering, Mysore 570 006, India*
[3]*Department of Studies in Physics, University of Mysore, Mysore 570 006, India*

Received 24 September 2003; accepted 12 April 2004
DOI 10.1002/app.20986
Published online in Wiley InterScience (www.interscience.wiley.com).

ABSTRACT: A series of polyurethane (PU)/poly(vinylidene chloride) (PVDC) interpenetrating polymer networks (IPNs) were synthesized through variations in the amounts of the prepolyurethane and vinylidene chloride monomer via sequential polymerization (80/20, 60/40, 50/50, 40/60, 30/70, and 20/80 PU/PVDC). The physicomechanical and optical properties of the IPNs were investigated. Thermogravimetric analysis (TGA) studies of the IPNs were performed to establish their thermal stability. TGA thermograms showed that the thermal degradation of the IPNs proceeded in three steps. Microcrystalline parameters, such as the crystal size and lattice disorder, of the PU/PVDC IPNs were estimated with wide-angle X-ray scattering.
 J Appl Polym Sci 103: 1375–1381, 2007

Key words: interpenetrating networks (IPN); mechanical properties; polyurethanes; thermogravimetric analysis (TGA)

INTRODUCTION

Castor oil is a naturally occurring vegetable oil; the presence of a secondary hydroxyl group and a double bond in ricinoleic acid has been exploited in versatile chemical syntheses.[1,2] A considerable amount of work has been done with castor-oil-based polyurethane (PU) interpenetrating polymer networks (IPNs).[3] A large number of commercial products have been developed with the concept of IPNs. IPNs are useful for designing materials with a wide variety of properties. An important commercial advantage is that IPNs offer a way of producing new materials with already existing polymers, thereby reducing development costs. Although there are many polymer blends, those containing halogenated polymers such as poly(vinyl chloride) (PVC) and poly(vinylidene chloride) (PVDC) are the most common commercial thermoplastics and are among the most important from both scientific and commercial points of view.[4–8] PVC is, therefore, often blended with other polymers,[9–12] including PU.[13–16]

PVDC polymers have been selected because of their excellent mechanical, thermal, and optical properties, fire resistance, weather resistance, and dimensional stability. A survey of the literature reveals that a lack of literature on IPNs of PU/PVDC. Novel IPNs of PU/PVDC will have well-define structures with PVDC pendant chlorine groups, which are assumed to stabilize the system thermally because of specific intramolecular and intermolecular interactions. In this research article, we report the structure–property relationship of PU/PVDC semi-IPNs.

EXPERIMENTAL

Materials

Castor oil was obtained from a local market, and its characteristic properties, such as the hydroxyl number (160–168), acid number (3.0), and isocyanate equivalent (330), were determined by standard procedures.[8] Other chemicals, such as methylene diisocyanate (MDI; Aldrich, Milwaukee, WI), benzoyl peroxide (BPO; Aldrich, Milwaukee, WI), and dibutyl tin dilaurate (DBTL; E.-Merck, Switzerland) were analytical-grade and were used without further purification. Vinylidene chloride (S.D. Fine Chemicals, Ltd., India) was freed from a stabilizer before use.

Synthesis of PU/PVDC IPNs

The prepolyurethane was synthesized with castor oil and MDI with an NCO/OH ratio of 1 : 1.4. PU/PVDC IPNs were synthesized through variations in the amounts of the prepolyurethane and vinylidene chloride monomer (80/20, 60/40, 50/50, 40/60, 30/70, and

Correspondence to: Siddaramaiah (siddaramaiah@yahoo.com).

20/80 PU/PVDC). PU/PVDC IPNs were synthesized via the charging of PU in different proportions into a 250-mL, three-necked, round-bottom flask. To this mixture, the calculated amount of the vinylidene chloride monomer, 0.5% BPO as an initiator, and 0.5% DBTL as a catalyst were added. The mixture was stirred at room temperature for 15 min to form a homogeneous solution. The reaction mixture was poured into a cleaned glass mold, which was sprayed with the releasing agent. The reaction was allowed to run at room temperature for 10 h. The temperature was then raised to 80°C to initiate vinylidene chloride polymerization. The mixture was kept at the same temperature for 10 h. The tough, golden yellow, transparent IPN films thus formed were cooled slowly and removed from the mold with different PU/PVDC compositions.

Techniques

The density and surface hardness were measured according to ASTM D 792 and ASTM D 785, respectively. The tensile behavior was measured according to ASTM D 882 with a Hounsfield (United Kingdom) 50 KN universal testing machine under ambient conditions. At least six samples were tested for each composition, and the average value was reported. The chemical resistivity of the IPNs was determined according to ASTM D 543-87. The selection of testing conditions considered the manner and duration of the contact with reagents, the temperature of the systems, and other performance factors involved in the particular applications.[17] Optical properties such as the transmittance and haze were measured according to ASTM D 1003 with a Suga (Japan) 206 test haze meter. The optical properties were recorded for dust- and grease-free thin IPN films.[18]

The thermal analysis of the IPNs was carried out with a Metler Polymerchemic Marburg FB 14 thermogravimetry instrument with the thermogravimetry module. The thermogravimetric analysis (TGA) scans were carried from 30 to 800°C at a heating rate of 20°C/min under a nitrogen atmosphere. The relative thermal stability of the PU/PVDC IPNs was evaluated through a comparison of the decomposition temperatures at various weight losses and the integral procedural decomposition temperature (IPDT). IPDT is defined as a means of summing up the whole shape of the normalized TGA data curve. IPDT, an index of the thermal stability, was determined from the thermogram area with a method reported in the literature.[19]

X-ray profile analysis

X-ray powder patterns of IPNs were recorded with a Philips PW 1140 diffractometer with Bragg–Branto geometry (fine-focus setting) with germanium monochromated radiation of Co Kα ($\lambda = 0.179$ nm) for a 2θ range of 5–50° at intervals of 0.03°; a curved position-sensitive detector was used in the transmission mode. These patterns were indexed with the Trial and Error Method (TREOR) procedure. The intensity was corrected for Lorentz polarization factors and also for instrumental broadening with the Stokes deconvolution method.[20]

Because each of the Bragg reflections in these samples, called the (*hkl*) reflections, broadened on account of crystal imperfections, we used profile analysis techniques to quantify these imperfections. Normally, the broadening of a profile arises because of the limited number of unit cells, called the crystal size ($\langle N \rangle$), counted in a direction perpendicular to the Bragg planes (*hkl*) and a disorder of second kind, called the lattice strain [g (%)]. This is given by $\Delta d/d$, where Δd is the change in the interplanar spacing and d is the interplanar spacing. It is possible to simulate an intensity profile with Hosemann's one-dimensional linear paracrystalline model, and the equation used for this purpose follows.[21]

The scattered intensity [$I(s)$] is

$$I(s) = 1_{N-1}(s) + 1'_N(s) \quad (1)$$

where s is equal to $2\pi \sin(\theta)/\lambda$, $I_{N-1}(s)$ is the scattered intensity calculated up to $(N-1)$ cells, and $I'_N(s)$ is the modified intensity for the probability peak centered at $D = Nd$ [N is the number of unit cells counted in a direction perpendicular to the (*hkl*) Bragg plane[22,23]]. $I_{N-1}(s)$ is computed as follows:

$$1_N(s) = 2Re\{(1 - I^{N+1})/(1 - I) + I_v/D(1 - I)^2[I^N(N(1 - I) + 1) - 1]\}^{-1} \quad (2)$$

where v is equal to $2ia^2s + d$, I is equal to $I(s) = \exp(-a^2s^2 + ids)$, $I_N(s)$ is the scattered intensity calculated due to the last cell, Re is the real part, and a^2 is equal to $\omega^2/2d$.

By substituting D, we obtain

$$I'_N(s) = (2a_N/D\pi^{1/2})\exp(iD_s)\{1 - a_Ns[2D(a_Ns) + i/\pi^{1/2}\exp(-a_Ns^2)]\} \quad (3)$$

where a^2_N is equal to $N\omega^2/2$ and $D(a_Ns)$ is Dawson's integral or the error function with a purely complex argument. g is given by $\Delta d/d = \omega/d$. For the computation of these three equations, the inputs were the experimental profile data, $\langle N \rangle$, and g. A SIMPLEX program was used to minimize the difference between the experimental and simulated profiles.[23]

The values of $\langle N \rangle$ and g were obtained for X-ray reflection at various 2θ angles. Here d_{hkl} is the perpendicular distance from the origin to the *hkl* plane, and ω is the standard deviation of the probability distribu-

TABLE I
Physicomechanical Properties of PU/PVDC IPNs

PU/PVDC	Density (g/cc, ±1%)	Tensile strength (MPa, ±2%)	Elongation at break (1; ±1%)	Tensile modulus (MPa, ±2%)	Surface hardness (±2%)	
					Shore A	Shore D
80/20	1.401	0.9	52	2.2	80	32
60/40	1.333	2.8	62	8.5	82	34
50/50	1.302	18.0	85	35.0	82	34
40/60	1.208	8.0	47	25.0	90	48
30/70	1.193	7.2	34	33.3	82	33
20/80	1.110	4.5	33	36.7	84	36

tion associated with the distortion of the lattice and is related to the strain by $g^2 = (\omega/d)^2$. s_0 is the scattering vector corresponding to the peak of the X-ray profile. The surface-weighted (D_{sur}) or volume-weighted (D_{vol}) crystal size is given by the integral:[24]

$$\langle D \rangle_{s,v} = \frac{LP_{sv}(L)dL}{LP_{sv}(L)dL} \tag{4}$$

and

$$P_s(L) = \alpha \frac{d^2A_s(n)}{dL^2} \tag{5}$$

where α is the width of the crystal size distribution. The volume-weighted column length distribution function $[P_v(L)]$ is given by $P_v(L) = \alpha L[\delta^2 A_s(n)/\delta L^2]$, where L is equal to nd_{hkl} and n is the harmonic number.[25]

RESULTS AND DISCUSSION

Physicomechanical properties

The calculated physicomechanical properties, such as the density, surface hardness, tensile strength, elongation at break, and tensile modulus of all the PU/PVDC compositions are given in Table I. The density of the PVDC homopolymer was 1.66–1.90 g/cc. The density increased with increasing PVDC content in the IPNs. This was due to denser PVDC being incorporated into the PU matrix.[26,27] The density values of IPNs lay in the range of 1.110–1.401 g/cc. The surface hardness values of PU/PVDC IPNs lay in the range of 80–88 (Shore A) and 32–48 (Shore D). The dimensional stability of the IPNs increased with an increase in the PVDC concentration. This was due to an increase in the plastic phase in the IPNs.

The mechanical properties are very important in selecting a polymer material for suitable applications. There was no systematic trend in the tensile strength with the PU/PVDC composition. Table I shows that the tensile strength increased as the PVDC concentration increased up to 50 wt %. A further increase in the PVDC content in the IPNs reduced the tensile strength. The reason for this may be the better interpenetration between the two polymers at the 50/50 PU/PVDC weight ratio in comparison with the other ratios.[28,29] The elongation and tensile modulus showed the same trend as the tensile strength. This indicated that the 50/50 PU/PVDC composition was the best for achieving maximum mechanical properties.[28,30]

Chemical resistance

It was very interesting to study the effects of the chemical environment on the IPNs in various solvents.[31] The IPN specimens were exposed to different chemical environments, including H_2O_2, HCl, NaCl, NaOH, $KMnO_4$, CCl_4, acetic acid, and water.[17] Each sample was dried, weighed, and soaked in different chemical reagents until absorption equilibrium was

TABLE II
Weight Change (%) of IPNs from Treatments with Different Chemical Reagents After 7 Days

PU/PVDC	10% NaOH	10% HCl	10% CH_3COOH	10% H_2O_2	10% NaCl	10% $KMnO_4$	CCl_4	H_2O
80/20	1.49	2.99	5.10	3.69	1.11	4.71	51.4	1.25
60/40	1.86	1.86	4.30	2.21	1.42	5.21	86.2	0.88
50/50	2.22	0.77	1.76	2.27	0.89	2.63	38.2	0.68
40/60	1.96	1.76	0.84	1.58	1.22	3.32	84.4	0.43
30/70	1.20	1.23	1.99	1.75	0.99	2.94	40.6	0.29
20/80	0.83	0.0	0.08	0.25	0.39	6.47	39.3	0.24

TABLE III
Optical Properties of PU/PVDC IPNs

PU/PVDC	Total transmittance (%)	Total diffusion (%)	Parallel (%)	Haze (%)
80/20	76	16.8	59.2	20
60/40	81	20.0	61.0	24
50/50	77	30.6	46.4	36
40/60	77	18.7	58.3	33
30/70	79	23.0	56	30
20/80	80	24.0	56	18

achieved, and this was followed by drying and reweighing in the absorbed state. The changes in the weight percentages of the PU/PVDC IPNs were determined in different chemical environments, and the results are listed in Table II. There was almost no significant change in the physical appearance of all the IPNs in all the chemical reagents under investigation. The IPNs were insoluble in many of the chemical reagents. The IPNs showed little resistance to alkali but much resistance to acids. The same trend was reported by Pattnaik and Nayak[32] for different PU IPNs.

Optical properties

Optical properties, such as the total transmittance, total diffusion, parallel, and haze percentages, of the IPNs are given in Table III. All the IPNs were very good transparent films, and the transmittance was 76–91%.[18,29] This was due to the good optical clarity of both the PU and PVDC films. Moreover, the haze values were 18–36%. There was no systematic variation in the optical properties because of the complicated chemical structure and morphology of the IPNs.[18,29]

TGA

TGA and derivative thermogravimetry (DTG) thermograms for the PU/PVDC (50/50) IPNs are shown in Figure 1. The TGA thermograms of all the IPNs are given in Figure 2. The thermograms obtained during TGA scans were analyzed to determine the weight-loss percentage as a function of temperature. T_0 (temperature of the decomposition onset), T_{10} (temperature of the 10% weight loss), T_{20} (temperature of the 20% weight loss), and T_{50} (temperature of the 50% weight loss) were the main criteria indicating the thermal stability of the IPNs (Table IV). The higher T_0, T_{10}, T_{20}, and T_{50} were, the higher the thermal stability was of the IPNs. Figure 2 shows that the TGA thermogram of the IPNs were stable up to 254°C and completely degraded around 539°C. The temperature range of decomposition, the weight-loss percentage, and the ash percentage are given in Table V. The IPNs showed a slow initial weight loss in the temperature range of 254–350°C, which is termed the first stage of the thermal degradation process. The weight loss in this step was 22–27%. The weight loss in this step was attributed to the loss of moisture, linear aliphatic hydrocarbons of castor oil, oligomers, and so forth. The second step of thermal degradation was in the range of 343–432°C, with a major weight loss of 24.4–31.7%. The weight loss in this step was assigned to the thermal degradation of linear PVDC and/or pseudo IPNs. The weight loss in the third stage was in the range of 430–520°C, with a weight loss of 15.8–26.9%. The weight loss that occurred in the third step of thermal degradation indicated the complete decomposition of the crosslinked IPNs.

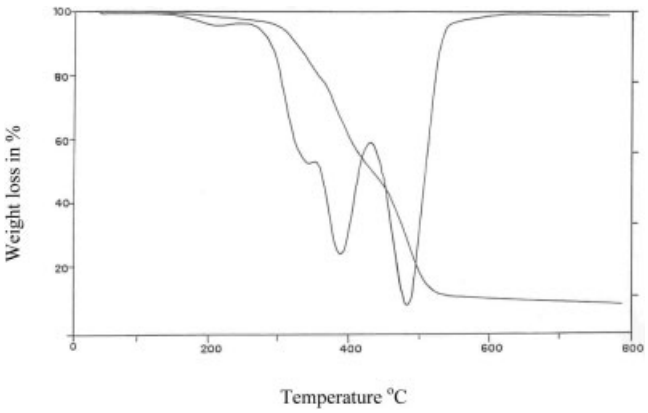

Figure 1 TGA and DTG curves of a 50/50 PU/PVDC IPN.

The relative thermal stability of the IPNs was evaluated by a comparison of the decomposition temperature at various weight losses. The IPDT was an index of the thermal stability of the system and was determined from the thermograms with a method reported in the literature.[19] Table IV shows that there was no change in the degradation pattern with the IPN com-

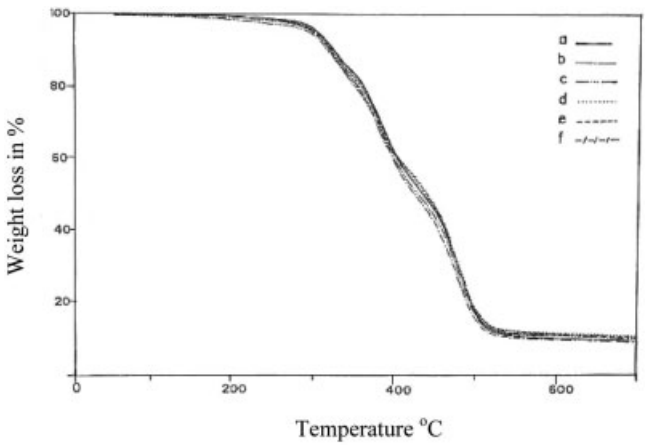

Figure 2 TGA curves of all the PU/PVDC IPNs.

TABLE IV
Characteristic Transition Temperatures Obtained from TGA Thermograms of PU/PVDC IPNs

PU/PVDC	Transition temperature (°C) up to various weight losses (±2%)				IPDT (°C; ±2%)
	T_0	T_{10}	T_{20}	T_{50}	
80/20	259	327	361	439	448
60/40	268	329	366	429	456
50/50	263	321	354	429	473
40/60	257	325	364	436	459
30/70	254	321	354	439	466
20/80	268	318	354	439	476

position. This was probably due to the thermal degradation patterns of PU and PVDC being almost identical. Table IV also shows that IPDT slightly increased with an increase in the PVDC content and was in the range of 448–476°C. This may have been due to an increase in the halogenated polymer content in the IPNs.

X-ray profile analysis

Wide-angle X-ray diffractometry studies were carried out for selected PU/PVDC IPNs in the 2θ range of 5–50°. X-ray diffractograms for 30/80, 40/60, 50/50, and 60/40 PU/PVDC IPNs are given in Figure 3. All the X-ray diffractograms show a small and broad peak, except for 50/50 PU/PVDC IPN; its diffractogram shows multiple sharp peaks in the 2θ range of 10.5–32°. This is due to the higher degree of crystallinity in this composition.

For the sake of completeness, we have reproduced in Figure 4 the experimental and simulated X-ray profiles for 30/80, 40,60, 50/50, and 60/40 PU/PVDC IPNs. The goodness of fit was less than 2% in all the samples, and this showed that the model used here was quite reliable.

TABLE V
Data Obtained from TGA Thermograms of PU/PVDC IPNs

PU/PVDC	Process	Temperature range (°C; ±2%)	Weight loss (%; ±2%)
80/20	1	259–346	14.7
	2	346–432	33.3
	3	432–559	41.1
	Ash	—	10.9
60/40	1	268–346	13.9
	2	346–432	36.4
	3	432–557	38.8
	Ash	—	10.9
50/50	1	263–350	17.8
	2	350–429	31.0
	3	429–550	38.8
	Ash	—	12.4
40/60	1	257–346	15.5
	2	346–427	31.0
	3	427–545	41.1
	Ash	—	12.4
30/70	1	254–348	17.1
	2	348–425	30.3
	3	425–543	40.5
	Ash	—	12.1
20/80	1	268–343	17.1
	2	343–420	27.2
	3	420–539	43.6
	Ash	—	12.1

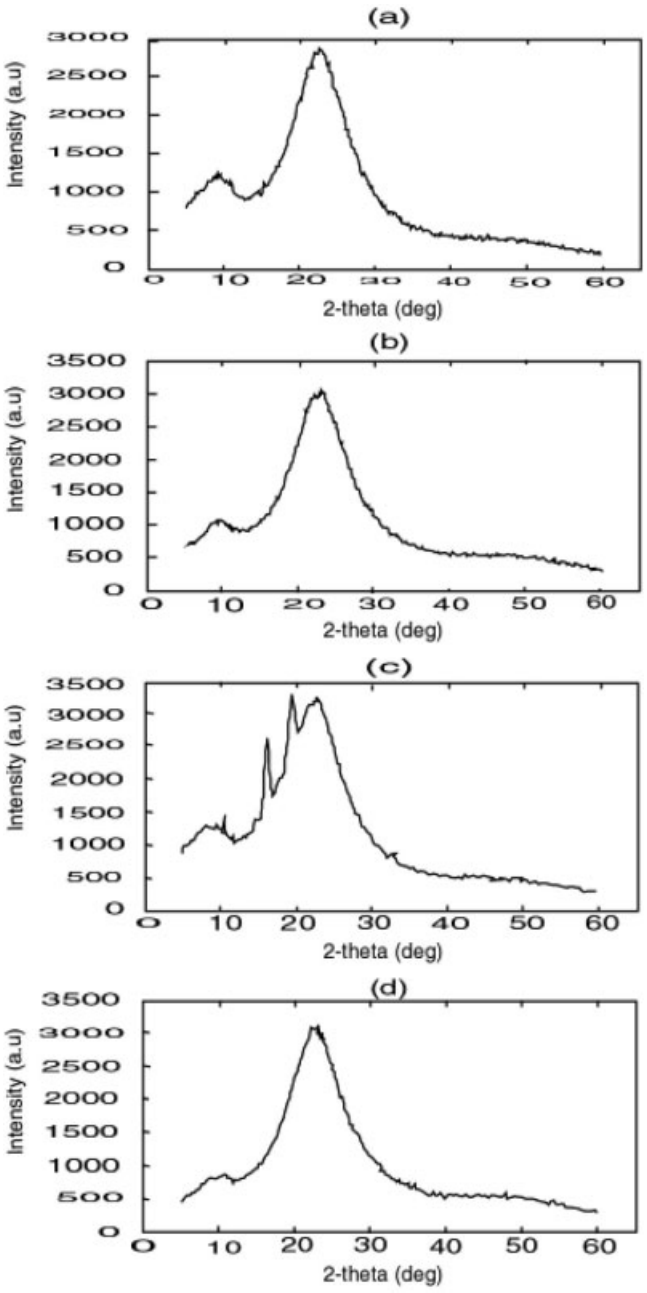

Figure 3 X-ray diffraction patterns of the PU/PVDC IPNs: (a) 30/70, (b) 40/60, (c) 50/50, and (d) 60/40.

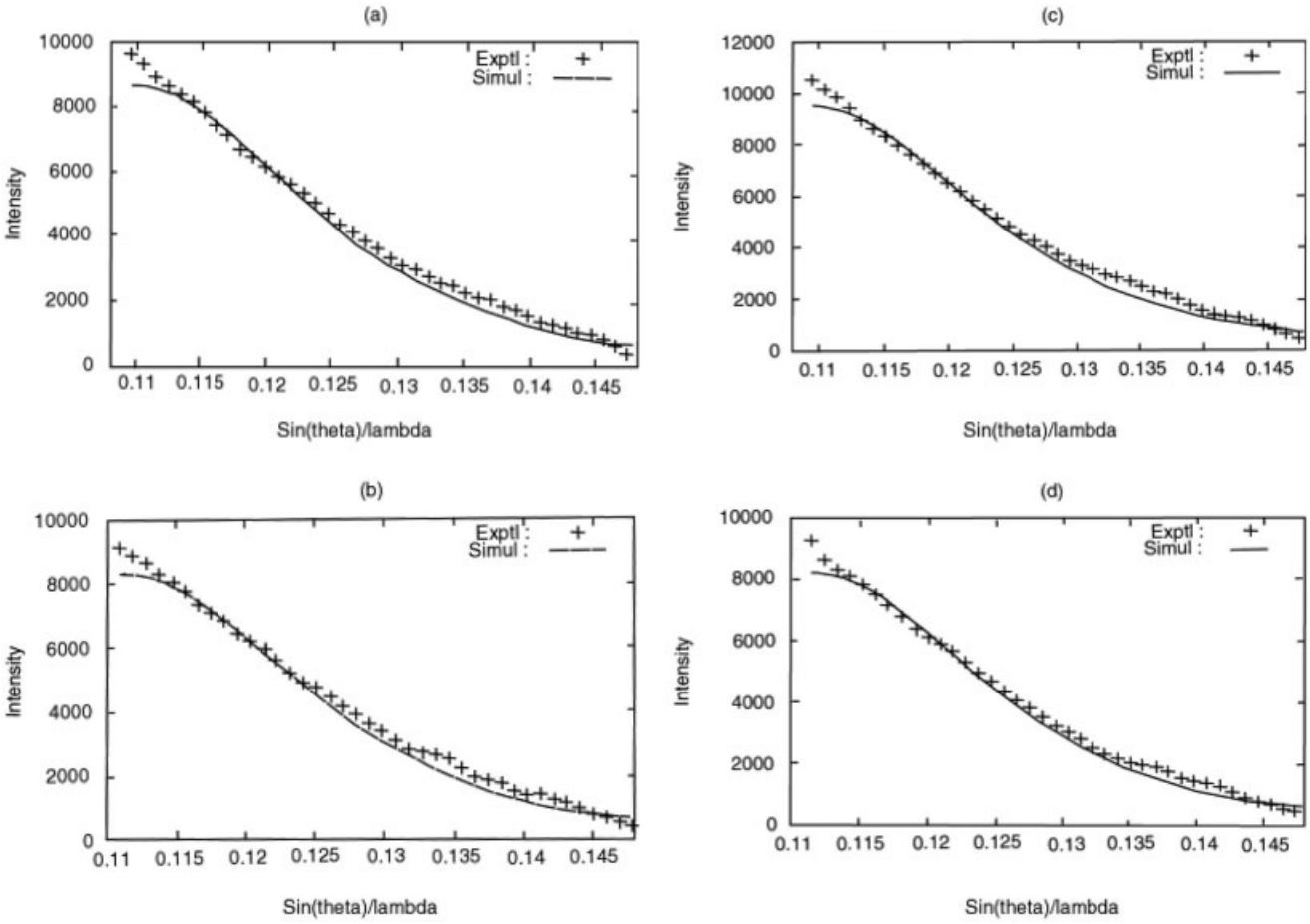

Figure 4 Experimental and simulated X-ray profiles of the PU/PVDC IPNs: (a) 30/70, (b) 40/60, (c) 50/50, and (d) 60/40.

The calculated microcrystalline parameters, such as $\langle N \rangle$, α, the smallest crystal unit (þ), g, and the enthalpy (α^*), for PU/PVDC IPNs are given in Table VI.

There was no systematic variation of $\langle N \rangle$, þ, g, and D_{sur} values with the composition of the IPNs. D_{sur} clearly indicated the extent of crystallinity present in the surface. A physical interpretation of crystal imperfection parameters such as $\langle N \rangle$ and g^{33} essentially indicated the deviation in the lattice ordering for a distance of $D = Nd_{hkl}$ (Å) along the direction normal to the Bragg (hkl) plane. Higher values of $\langle N \rangle$, P, and D_{sur} were observed for 50/50 PU/PVDC in comparison with other IPN systems. This result was consistent with the physicomechanical properties of the IPNs.

Phase stabilization occurred in all the PU/PVDC IPNs. This conclusion was drawn from the minimum value of α^* (0.01–0.03), a measure of the energy required for the formation of a net plane structure. Here α^* physically indicated that the growth of the paracrystals in a particular material was appreciably controlled by the level of strain (g) in the net plane structure. The calculated interplanar spacing (d_{hkl}), given in Table VI, lay in the range of 4.43–4.49 Å. These values were almost identical for all IPNs. Tables I and VI show that there was a significant change in $\langle N \rangle$ of the IPNs with the composition, and this resulted in a nonlinear variation of the physicomechanical properties with the crystal size parameters.

TABLE VI
Microstructural Parameters of PU/PVDC IPNs

Composition	2θ (°)	$\langle N \rangle$	Å	α	g (%)	α^*	D_s (Å)	d_{hkl} (Å)
20/80	22.60	2.58 ± 0.17	1.71	1.51	2.0 ± 0.1	0.03	11.78	4.49
40/60	22.89	2.71 ± 0.18	1.80	1.11	1.0 ± 0.1	0.02	12.22	4.43
50/50	22.60	2.58 ± 0.17	1.62	1.04	1.5 ± 0.1	0.02	11.78	4.49
60/40	23.00	2.80 ± 0.19	1.83	1.03	0.5 ± 0.1	0.01	12.56	4.41

CONCLUSIONS

The following conclusions can be drawn from this investigation:

1. Tough, good, and transparent PU/PVDC semi-IPNs were synthesized. The transparency values were 77–91%.
2. The optimized composition for achieving maximum mechanical performance was 50/50 PU/PVDC.
3. The thermal stability of all the PU/PVDC IPNs was greater than 254°C; they completely degraded at 539°C.
4. TGA curves showed three significant thermal degradation steps at approximately 254–350, 343–432, and 420–559°C. They were due to the complicated chemical structure and morphology of the IPNs.
5. An X-ray profile analysis of the PU/PVDC systems revealed that the changes in the physical properties were essentially attributed to the rearrangement of the polymer network, with a new set of microstructural parameters computed with broadened profiles. X-ray data revealed that these IPNs were semicrystalline in nature.

The complete morphological and structural description of a PU/PVDC IPN is extremely complex because both PVDC, with its hierarchical microstructure arrangement, and PU, with alternate soft and hard segment units, contribute to the multicomponent blend system, thus affecting considerably its mechanical and thermal properties.

References

1. Cassidy, P. E.; Schwank, G. D. J Appl Polym Sci 1974, 18, 2517.
2. Achaya, R. T. J Am Oil Soc 1971, 48, 762.
3. Barret, L. W.; Sperling, L. H. Polym Eng Sci 1991, 33, 913.
4. Braun, D.; Kommerling, S. Angew Makromol Chem 1992, 195.
5. Vorenkemp, E.; Brinke, G.; Meijer, J. G.; Jager, H.; Challa, G. Polymer 1985, 14, 1725.
6. Shen, S.; Torkelson, J. M. Macromolecules 1992, 25, 721.
7. Varnell, D. F.; Moskala, E. J.; Painter, P. C.; Coleman, M. M. Polym Eng Sci 1983, 23, 658.
8. Fowkes, F. M.; Tischler, D. O.; Wolfe, J. A.; Lannigan, L. A.; Ademu-John, C. M.; Halliwell, M. J. J Polym Sci Polym Phys Ed 1984, 22, 547.
9. Parmer, F. F.; Dickinson, L. C.; Chien, J. C. W.; Porter, R. S. Macromolecules 1989, 22, 1078.
10. Tremblay, C.; Prud'homme, R. E. J Polym Sci Polym Phys Ed 1984, 22, 1857.
11. Handbook of Polymer Degradation; Hamid, S., Ed.; Marcel Dekker: New York, 1992.
12. Allen, G.; Bevington, J. Comprehensive Polymer Science; Pergamon: Oxford, 1989; Vol. 6.
13. Piglowski, J.; Laskawski, W. Angew Makromol Chem 1979, 82, 157.
14. Kalfoglou, N. K. J Appl Polym Sci 1981, 26, 823.
15. Lavallee, J.; Carmel, M.; Utracki, L. A.; Szabo, J. P.; Keough, I. A.; Favis, B. D. Polym Eng Sci 1992, 32, 1716.
16. Haponiuk, J. T.; Balas, A. J Therm Anal 1995, 43, 215.
17. Sperling, L. H.; Mihalakis, E. N. J Appl Polym Sci 1973, 17, 3811.
18. Patel, P.; Shah, T.; Suthar, B. J Polym Mater 1988, 6, 193.
19. Doyle, C. D. Anal Chem 1961, 33, 77.
20. Stokes, A. R. Proc Phys Soc London 1948, 61, 382.
21. Wilson, A. J. C. Elements of X-Ray Crystallography; Addison-Wesley: Reading, MA, 1970; p 191.
22. Numerical Recipes; Press, W.; Flannery, B. P.; Tenkolsley, S.; Velterling, W. T., Eds.; Cambridge University Press: Cambridge, England, 1986; p 83.
23. Silver, M. M.S. Thesis, UMIST, 1998.
24. Balzar, D. J Res Natl Inst Stand Tech 1993, 88, 32.
25. Somashekar, R.; Somashekarappa, H. J Appl Crystallogr 1997, 30, 147.
26. Raut, S.; Athawale, V. Eur Polym J 2000, 36, 1379.
27. Millar. J Chem Soc 1960, 1311.
28. Bai, S.; Khakhar, D. V.; Nadkarni, V. M. J Polym Sci 1997, 38, 1319.
29. Suthar, B.; Parikh, N.; Patel, N. Polym Int 1991, 25, 175.
30. Ramesh, P.; Rajalingam, P.; Radhakrishnan, G.; Francis, D. J. Met Mater Process 1989, 1, 197.
31. Zap, R. L. Polym Prepr 1970, 11(1), 358.
32. Pattnaik, T.; Nayak, P. L. Macromol Rep A 1994, 31, 447.
33. Warren, B. E.; Averbach, B. L. J Appl Phys 1950, 21, 595.